Kinetics of the Gas-Phase Addition of the Ethyl Radical and the *tert*-Butyl Radical to NO

Herbert Dilger, Martina Stolmár, Ulrich Himmer, and Emil Roduner*

Institut für Physikalische Chemie, Pfaffenwaldring 55, D-70569 Stuttgart, Germany

Ivan D. Reid

Paul Scherrer Institute, CH-5232 Villigen PSI, Switzerland

Received: February 11, 1998; In Final Form: June 17, 1998

The kinetics of the addition reaction of the ethyl radical and the *tert*-butyl radical to NO has been investigated at 1.5 bar as a function of temperature (219−475 K) using the muon spin relaxation technique in longitudinal magnetic fields. The data are represented by $k_1 = (4.5^{+4.1}_{-2.1}) \times 10^{-10}\ T^{-0.5\pm0.1}$ cm^3 molecule^{-1} s^{-1} for the ethyl radical and $k_2 = (5.2^{+8.3}_{-3.1}) \times 10^{-4}\ T^{-3.1\pm0.2}$ cm^3 molecule^{-1} s^{-1} for the *tert*-butyl radical, or alternatively by Arrhenius parameters of $E_a = -(1.4 \pm 0.3)$ kJ mol^{-1} and $A = (1.3 \pm 0.2) \times 10^{-11}$ cm^3 molecule^{-1} s^{-1} for the ethyl radical and of $E_a = -(7.3 \pm 0.4)$ kJ mol^{-1} and $A = (5.5 \pm 0.9) \times 10^{-13}$ cm^3 molecule^{-1} s^{-1} for the *tert*-butyl radical. They provide a basis for tests of absolute rate theories for reactions occurring on more than one potential energy surface.

Introduction

During recent years, the influence of atmospheric pollutants on climate and health has attracted much public interest. Organic free radicals are important intermediates in pyrolysis, oxidation, and photochemical reactions, and they therefore play a key role in the degradation of organic pollutants and in combustion processes.[1] There is a complex interplay between reactions, each with its own pressure and temperature dependence. In the interest of a clean atmosphere and in order to reduce the consumption of fuels, computer modeling aims at a better understanding of these processes, but accurate kinetic parameters are necessary for such calculations.

Muon spin relaxation (μSR) was recently used successfully to study spin exchange and chemical reactions of the ethyl radical and of the *tert*-butyl radical with oxygen.[2,3] The technique, a variant of magnetic resonance, uses spin-polarized positive muons as spin labels. Available at the beam ports of suitable accelerators, the muons are stopped in an experimental target. After thermalization a muon captures an electron to form muonium (Mu ≡ μ^+e^-), which is chemically a light isotope of hydrogen with a positive muon as its nucleus. Muonium then adds to an unsaturated bond of the alkene that is present in the reaction vessel. This places the muon in a radical where it serves as a highly polarized spin label. A detailed description of the technique has been given elsewhere.[4,5]

In the present work the technique was used to investigate the reactions

$$\dot{C}H_2CH_2Mu + NO \xrightarrow{[M]} CH_2(CH_2Mu)NO \qquad (1)$$

and

$$(CH_3)_2\dot{C}CH_2Mu + NO \xrightarrow{[M]} (CH_3)_2C(CH_2Mu)NO \qquad (2)$$

where $\dot{C}H_2CH_2Mu$ is the muonium substituted ethyl radical and $(CH_3)_2\dot{C}CH_2Mu$ the muonium-substituted *tert*-butyl radical. M is a moderator molecule (here N_2), which takes over the excess energy of the transition state. The muonium-substituted ethyl radical is generally formed by addition of the muonium atom to ethene,[6] and $(CH_3)_2\dot{C}CH_2Mu$ is formed by addition of muonium to isobutene.[6,7] Reactions with NO are important in the troposphere, where the NO levels are elevated.[8]

Accurate experimental kinetic data are also the basis for further developments of reaction rate theories. Since the reactions R + O_2 (R = $\dot{C}H_2CH_2Mu$, $(CH_3)_2\dot{C}CH_2Mu$) have been investigated earlier, the work was extended to R + NO. The reactions R + O_2 seem to obey simple correlations with ionization potentials and electron affinities,[9] but those of radicals with NO are more complicated. In the present context the most simple reaction is the addition of the methyl radical to NO, for which extended theoretical and experimental investigations have been performed by Davies et al.,[10] Pratt et al.,[11] and Kaiser.[12] Here, the association can take place on more than one potential-energy surface. The orbital degeneracy of the ground state of NO, coupled with the 2-fold spin degeneracy of each of the two reacting species, leads to a correlation with four electronic states of the product. The complications of such systems have been discussed in detail by Smith.[13]

The reaction of the ethyl radical with NO has been investigated by Pratt et al. at room temperature,[11,14] but the rate constant is about two orders of magnitude lower than that of the reaction of the methyl radical with NO. There is no obvious reason for such a difference, so that a reassessment of the problem is justified. The reaction of the *tert*-butyl radical with NO has, to our knowledge, not been measured so far.

The electronic potential energy on at least the lowest electronic surface usually falls monotonically as the distance between the radicals is reduced. Therefore the probability of reaction on the long-range attractive potential will decrease for increasing collision energy between the radicals. This, together

* Corresponding author; e-mail: roduner@indigo01.chemie.uni-stuttgart.de.

S1089-5639(98)01101-3 CCC: $15.00
Published on Web 07/31/1998

with changes in reagent rotational energy, may lead to rate constants that decrease as the temperature is raised.[13]

Standard methods of magnetic resonance are less useful for gas-phase investigations of radicals with more than three or four atoms, since the number of resonances increases strongly with the number of atoms. Other methods such as UV absorption spectroscopy or mass spectroscopy are limited by their sensitivity and by time resolution, and radical concentrations of the order of 10^{11} molecules cm^{-3} are necessary. Self-terminations of the radicals occur and have to be taken into account. In the μSR technique, in contrast, only a single radical exists at a time in the reactor; therefore, no self-termination occurs.

Experimental Technique and Data Analysis

Muon Production and Decay. All experiments were carried out using "surface" muons of 4.1 MeV energy from the πE3 beam line at the Paul Scherrer Institute (PSI) in Villigen, Switzerland. To produce polarized muons, a proton beam is accelerated to an energy of approximately 600 MeV and focused onto a graphite target. Nuclear reactions result in the production of positive pions (π^+). With a lifetime of 26 ns, these particles decay at rest at the surface of the target according to

$$\pi^+ \rightarrow \mu^+ + \nu_\mu \tag{3}$$

into a positive muon (μ^+) and a neutrino (ν_μ), which are both spin-$^1/_2$ particles. This is a parity-violating decay, with neutrino helicity of -1, which means that the spin of the neutrino is exactly opposite to its momentum. Owing to conservation of spin and linear momentum, both zero for the pion at rest, the muons are polarized opposite to their momentum as well. By selecting these muons in a small solid angle, a muon beam with a spin polarization close to 100% is produced. Having a lifetime of $\tau_\mu = 2.2$ μs, the muon decays according to

$$\mu^+ \rightarrow e^+ + \bar{\nu}_\mu + \nu_e \tag{4}$$

into a positron and two neutrinos, again a parity-violating process. The decay positron is emitted preferentially along the direction of the muon spin. In the experiment, these decay positrons are counted using two sets of detectors, which are placed parallel and antiparallel to the initial muon polarization.

In time differential mode used in this work the spin-polarized muon first passes a thin detector, where it loses part of its energy and triggers a start signal of a time digitizer before entering the reaction vessel. The muon then slows down in the gas mixture and forms Mu by a charge exchange process. Addition to the alkene leads to the desired Mu-substituted radical. When the decay positron hits one of the positron detectors, a stop signal is produced. The event increments the counts in the channel corresponding to the time between start and stop signal. The number of these events plotted against the time difference is called μSR histogram.

Under stationary conditions the histogram shows a single-exponential decay with the muon lifetime τ_μ. In the presence of relaxation due to spin exchange, spin rotation interaction, or chemical reaction processes, the form of the histogram is given by

$$N(t) = \mathrm{BG} + N_0 e^{-t/\tau_m}[1 + AP(t)] \tag{5}$$

where BG represents a constant background and N_0 is a normalization factor. The time evolution of the muon spin polarization is described by $P(t)$. The prefactor A contains the asymmetry of the muon decay and instrumental components.

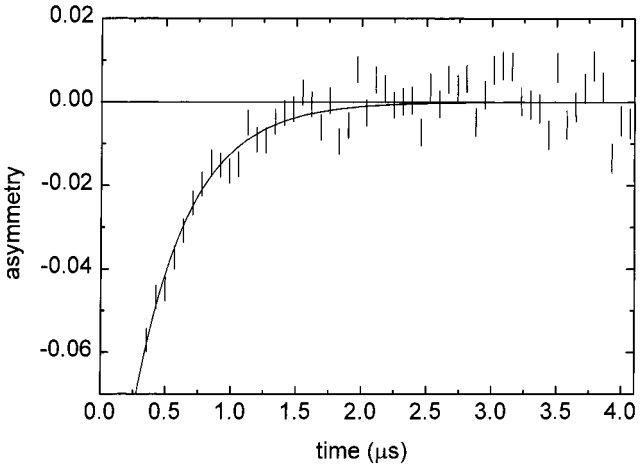

Figure 1. Asymmetry of a histogram obtained with a NO concentration of 8.3×10^{16} molecules cm^{-3} and an isobutene partial pressure of 156 mbar in N_2 (total pressure of 1.5 bar), a field of 0.1 T, and a temperature of 365 K. A single-exponential decay is observed. An exponential function with λ given by eq 6 is fitted to the data (solid line). The first 328 ns are not used because of distortions due to the electronics.

Two detector sets, one in the forward (F) and one in the backward (B) direction with respect to the muon momentum, are used for positron detection. The two time-resolved histograms derived from this configuration allow the muon spin relaxation to be monitored directly. Figure 1 shows the asymmetry $AP(t)$ a of a typical backward histogram.

Experimental Setup and Gas Handling. The reaction vessel, a cylinder of 500 mm length and 80 mm diameter, is placed in the horizontal bore of a superconducting magnet. A copper tube surrounding it allows heating and cooling of the gas by recirculating a temperature-regulated liquid. The magnetic field is parallel to the initial muon polarization and can be swept continuously between 0 and 5 T. Detailed information regarding the experimental apparatus can be found in an earlier paper.[2]

The gas was premixed in a 1-L mini-can, which was first filled with a known amount of NO. For the reaction of the ethyl radical with NO, it then was topped up with ethene to a pressure of 7 bar. This gas mixture was expanded into the reaction vessel, yielding a pressure of 1.5 bar. For the reaction of the *tert*-butyl radical with NO, 990 mbar of isobutene was first added to the NO. The mixture was then topped up with nitrogen to a pressure of 9.5 bar. After the gas mixture was expanded into the reaction vessel to a total pressure of 1.5 bar, the final partial pressure of isobutene was 156 mbar. Fresh NO with a nominal purity (as specified on the cylinder) of 99.0% and 99.5% for the ethyl radical and the *tert*-butyl radical, respectively, was used for all experiments.

Data Analysis. As derived in a previous work, the relaxation rate of the muon spins in a longitudinal field is given by[2]

$$\lambda = \lambda_0 + \lambda_{ch} + \frac{\lambda_{ex}}{2(1 + x^2)} \tag{6}$$

Here, λ_0 is the intrinsic relaxation rate in the radical, λ_{ch} the rate of chemical reaction given by eqs 1 and 2, and λ_{ex} the rate of electron spin exchange between the unpaired radical electron and NO. To derive the muon relaxation rate caused by spin exchange, λ_{ex} must be divided by a factor of $2(1 + x^2)$ to take into account the decoupling of the muon from the electron in high fields. x represents B/B_0, where B is the applied field and B_0 the muon-electron hyperfine coupling constant in magnetic

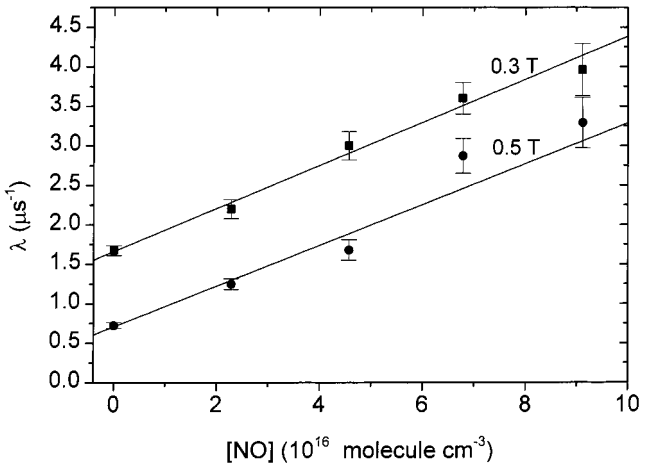

Figure 2. Muon spin relaxation rate for the reaction of the ethyl radical with NO at 243 K, plotted over the NO concentration at two different magnetic fields.

field units. For the ethyl radical, B_0 ranges between 12.4 mT at 243 K and 10.7 mT at 475 K,[15,16] and for the *tert*-butyl radical it is between 11.2 mT at 219 K and 9.7 mT at 408 K.[16,17] Since an experiment uses a total of $\sim 10^9$ muons only, the kinetics is of pseudo-first-order, so that $\lambda_{ex} = k_{ex}[NO]$ and $\lambda_{ch} = k_{ch}[NO]$. The polarization thus decays according to

$$\lambda = \lambda_0 + \left(k_{ch} + \frac{k_{ex}}{2(1+x^2)}\right)[NO] = \lambda_0 + k[NO] \qquad (7)$$

Equation 7 is the direct basis for the analysis of the experimental data. The quantities of interest are the bimolecular rate constants for spin exchange and for chemical reaction. We see that the inverse quadratic field dependence of spin exchange allows the separation of the two processes. This was verified for the reaction of the muonium-substituted ethyl radical with O_2[2] and for the collision of Mu with various other paramagnetic species.[18]

Data were analyzed using the MINUIT program package,[19] which minimizes χ^2 first by a SIMPLEX algorithm and after convergence with a gradient procedure. Analysis gives one standard deviation parabolic errors, and asymmetric errors in the case of correlated parameters.

Results

Time differential measurements with ethene were performed at several longitudinal magnetic fields and temperatures in the range 243 to 475 K. Figure 2 shows a typical series of results obtained at different concentrations of NO, at magnetic fields of 0.3 and 0.5 T. In the following we use k_1 for k_{ch} of reaction 1 and k_2 for k_{ch} of reaction 2.

The excellent linearity demonstrates that the increase of the relaxation rate is proportional to the NO concentration only. The intercepts represent the intrinsic relaxation (λ_0). These values agree well with those of previous determinations in the pure gas.[6,7,20] The slopes give the rate constants of the chemical reaction, and in principle a field-dependent contribution of spin exchange ($k_{ex}/2(1 + x^2)$). For the two magnetic fields the slopes are the same within error, which shows that the contribution of spin exchange must be small. As we know from other experiments,[2,3] spin exchange with O_2 is collision-controlled. The collision limit is given by $k_{coll} = \sigma(8kT/\pi m^*)^{1/2}$, where σ is the collision cross section and m^* the reduced mass of the colliding molecules. Using diameters of 0.44 nm for the ethyl radical and 0.35 nm for NO we obtain $k_{coll} = 2.0 \times 10^{-11}$ cm^3 molecule^{-1} s^{-1} K$^{-1/2}$(T)$^{1/2}$. This constant has to be divided by a factor of 2 for a spin-$^1/_2$ entity like NO to give k_{ex}.[18,21] For the highest temperature (475 K) and the lowest field (0.3 T) where spin exchange is fastest and the chemical reaction is slow, we obtain a maximum contribution of spin exchange of 1.2% ($k_{ex}/2(1 + x^2) = 1.4 \times 10^{-13}$ cm^3 molecule^{-1} s^{-1}). This is well within error of the experiment and can be neglected. The slopes, k_1(0.3T) and k_1(0.5T), are therefore averaged over the fields to yield the final rate constant for chemical reaction, k_1, as given in Table 1.

The reaction of the *tert*-butyl radical with NO was investigated in the temperature range of 219 to 408 K. Experiment and data analysis were carried out as for the ethyl radical. As seen in Figure 3, the relaxation rate shows a good proportionality to the NO concentration, and the slopes are equal within error. For a diameter of 0.52 nm for *tert*-butyl we obtain a collision limit of $k_{coll} = 2.1 \times 10^{-11}$ cm^3 molecule^{-1} s^{-1}(T)$^{1/2}$, which gives a contribution of spin exchange to k_2 of about 22% ($k_{ex}/2(1 + x^2) = 9.9 \times 10^{-13}$ cm^3 molecule^{-1} s^{-1}) for 0.1 T, 4% for 0.2 T, and 2% for 0.3 T at a temperature of 408 K. Since this is the maximum of all temperatures, and since the error bars of k_2 are larger than the expected contribution of spin exchange, even for the lowest field, this contribution was neglected as well.

The intercept at 0.3 T (this is the only field that was used for both reactions) is lower by a factor of 4 than for the ethyl radical. This is due to the higher moment of inertia of *tert*-butyl, which leads to a lower electron relaxation rate.[6,22] A list of the chemical rate constants for the reaction is given in Table 2.

Discussion

Rate Constants. For the discussion of the rate constants we refer to the Arrhenius plot in Figure 4. Arrhenius fits to the data are shown by solid lines. The collision limit of the ethyl reaction with NO is represented by the dashed−dotted line. A high-pressure extrapolation for the reaction of the methyl radical with NO is included as well.[10] Two lines (dashed and dotted) represent the results of two different analyses of the same data set.

In our earlier work we demonstrated that the rate constant for the reaction of the ethyl radical with O_2 has certainly reached its high-pressure limiting value at 1.5 bar[2]. A pressure dependence was not investigated in the present work, but since the reactions with O_2 and NO are very similar and since there are as many internal degrees of freedom in the radical as in the previous case, we have no reason to believe that the high-pressure limit has not been reached for the reactions with NO.

Ethyl Radical. An Arrhenius fit to the data results in a frequency factor of $A = (1.3 \pm 0.2) \times 10^{-11}$ cm^3 molecule^{-1} s^{-1} and an activation energy of $E_a = -(1.4 \pm 0.3)$ kJ mol^{-1}. This activation energy is negative as well but lower than for the reaction of $\dot{C}H_2CH_2Mu$ ($E_a = -(2.4 \pm 0.3)$ kJ mol^{-1}).[2] Negative activation energies are typical for addition reactions involving small species.[23] A second dependence derived from the Troe factorization that is often used in the literature is the $B \times T^n$ law. Fitting this to the rate constants results in $k_1 = (4.5^{+4.1}_{-2.1}) \times 10^{-10} T^{-0.5\pm0.1}$ cm^3 molecule^{-1} s^{-1}. Both representations are used here to keep the data compatible with literature. In absence of a detailed theory, we prefer the more conventional Arrhenius representation. k_1 is lower than the collision limit by a factor of 12−14. Since at 1.5 bar the reaction is expected to be close to the high-pressure limit, as was observed for the addition of O_2 to the ethyl radical,[2] this effect is expected to be related to the dynamics on the anisotropic potential surface,

TABLE 1: Rate Constants for the Chemical Reaction of the Ethyl Radical with NO at Different Temperatures[a]

	T (K)				
	243	260	319	387	475
k_1(0.3 T) (10^{-12} cm^3 molecule^{-1} s^{-1})	27.2 ± 2.1	21.8 ± 2.3	22.6 ± 2.0	20.7 ± 2.6	11.8 ± 3.3
k_1(0.5 T) (10^{-12} cm^3 molecule^{-1} s^{-1})	25.8 ± 1.8	22.4 ± 1.4	21.8 ± 1.5	18.2 ± 1.7	20.1 ± 2.0
k_1 (10^{-12} cm^3 molecule^{-1} s^{-1})	26.4 ± 1.4	22.2 ± 1.2	22.1 ± 1.2	19.0 ± 1.4	17.7 ± 1.7

[a] The lowest line contains the weighted average of the upper lines.

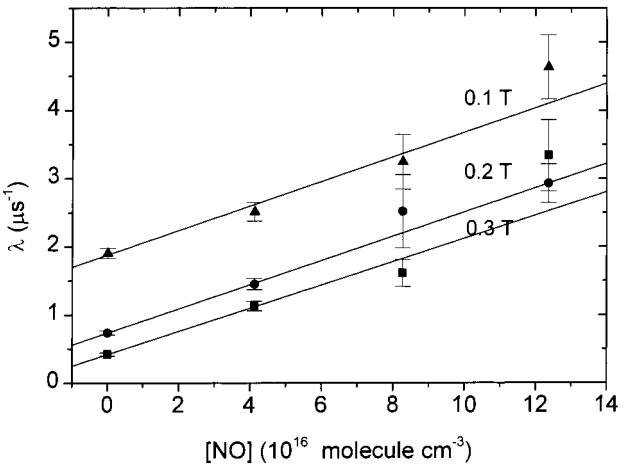

Figure 3. Rate of muon spin relaxation for the reaction of the *tert*-butyl radical with NO at 248 K, plotted over the NO concentration at three different magnetic fields.

which takes into account that not all directions of approach lead to successful bond formation with equal probability.

At room temperature the rate constant has a value of $k_1 = 2.3 \times 10^{-11}$ cm^3 molecule^{-1} s^{-1}, 100 times higher than the only comparable value of Pratt et al. ($k_1 = 2.3 \times 10^{-13}$ cm^3 molecule^{-1} s^{-1}, also obtained at room temperature).[11] Pratt found no pressure dependence in the range of 11−20 mbar and believed that their measurement was at the high-pressure limit,[11,14] but the range of pressures may have been too small to claim the high-pressure limit of the reaction. Our results compare well with those for the analogous reactions of the methyl and the *tert*-butyl radicals. Results for halogenated methyl + NO reactions give rate constants which are comparable to those in this work as well.[24] Thus, either the high-pressure limit must be higher than expected by Pratt et al. or their value is too low for other reasons.

***tert*-Butyl Radical.** The Arrhenius frequency factor is $A = (5.5 \pm 0.9) \times 10^{-13}$ cm^3 molecule^{-1} s^{-1} and the activation energy $E_a = -(7.3 \pm 0.4)$ kJ mol^{-1}, about 5.2 times more negative than for the reaction of the ethyl radical with NO. The $B \times T^n$ fit results in $k_2 = (5.2^{+8.3}_{-3.1}) \times 10^{-4}\ T^{-3.1\pm0.2}$ cm^3 molecule^{-1} s^{-1}. In the temperature range of observation, k_2 is below the collision limit by a factor of 10−81.

The *tert*-butyl radical has many more degrees of freedom for vibration and rotation than the ethyl radical, which makes distribution of energy and transfer to the moderator more efficient.[25,26] Therefore, the unusually high negative activation energy of the reaction cannot be explained by deviations from the high-pressure limit. Rather, the increase of the reaction rate and thus of the reaction cross section with decreasing temperature must again be related to the dynamics on the anisotropic potential surface, which makes soft glancing collisions more reactive at low temperatures.

Systematic Errors. Uncertainties of the compositions of the gas mixtures are estimated to be <5%. The statistical errors in our rate constants are of the order of 10%. The systems are homogeneous, chemically clean, and well-defined. Addition of ethyl or *tert*-butyl radicals to alkenes is too slow to make a significant contribution to the relaxation.[27] Self-termination reactions cannot occur because there is only a single muonated radical present at any time in the whole volume, and wall reactions are extremely improbable because the dimension of the gas cell is large compared with the diffusive displacement of the radical during the muon lifetime (∼1 mm). The kinetics is thus of ideal pseudo-first order, and $k_{1,2}$ represents the reaction with NO alone.

One possibility for a misinterpretation of the observed relaxation would be spin exchange or chemical reaction of the radical precursor muonium with NO.[28] In 1.5 bar ethene, muonium has a lifetime of ∼5 ns[29] so that its presence and the buildup of the ethyl radical do not interfere on the microsecond time scale. For the system of *tert*-butyl the muonium lifetime could be longer because the partial pressure of the isobutene was lower by a factor of 10 than the ethene pressure. On the basis of the rate constant of Mu addition to ethene,[29] we would expect a muon lifetime of ∼50 ns in the presence of 156 mbar isobutene. This is still short compared with the time window of our experiment (10 μs). Long-lived muonium would be indicated in a histogram as a second exponential decay of the muon polarization. Since this was not observed, we conclude that the buildup of the radical is faster than the dead time of the experiment for isobutene as well (Figure 1). The rate constant for Mu addition is probably larger for isobutene than for ethene.

We also have to consider a possible kinetic isotope effect due to the substitution of Mu for the more common hydrogen isotope. Since the bond to Mu is neither formed nor broken in the reaction of interest (eqs 1 and 2), we only have to consider a secondary isotope effect, which is normally small.[30] Statistical thermodynamics calculations based on the AM1 method[31] reveal that the addition reaction of the muonated ethyl radical to NO is by 0.1 kJ mol^{-1} less exothermic and has a 0.35 J mol^{-1} K^{-1} higher reaction entropy than the conventional H isotopomer. The reaction is exothermic by ∼160 kJ mol^{-1} [32] and presumably barrierless as for the reaction with O_2.[33] We therefore expect an early transition state that resembles the reactants, and a secondary isotope effect should cancel. A late transition state that resembles the products is not expected, but if it occurred the above reaction enthalpy and entropy would translate into a secondary isotope effect of at most 9% (slower for the Mu isotopomer).

For the reaction of *tert*-butyl with NO, the calculations reveal that the addition of the muonated isotopomer is less exothermic by 1.3 kJ mol^{-1} and has a 4.0 J mol^{-1} K^{-1} lower reaction entropy than the normal isotopomer. The reaction is again strongly exothermic so that we expect an early transition state and therefore a negligible kinetic isotope effect as in the previous case.

Interpretation of the Rate Constants. The mechanism of radical addition reactions has been of considerable recent interest in view of the influence of steric and polar electronic effects on reaction rates, which can vary by many orders of magnitudes,

TABLE 2: Rate Constants for the Chemical Reaction of the *tert*-Butyl Radical with NO at Different Temperatures[a]

	T (K)					
	219	248	273	295	350	408
k_2(0.1 T) (10^{-12} cm^3 molecule^{-1} s^{-1})	29.9 ± 4.1	18.0 ± 2.6	16.4 ± 1.9	12.0 ± 2.4	4.5 ± 1.6	4.5 ± 1.3
k_2(0.2 T) (10^{-12} cm^3 molecule^{-1} s^{-1})	33.8 ± 2.6	17.8 ± 0.7	14.8 ± 0.8	11.0 ± 1.7	6.2 ± 0.6	6.5 ± 1.1
k_2(0.3 T) (10^{-12} cm^3 molecule^{-1} s^{-1})	27.8 ± 2.9	18.0 ± 2.6	14.5 ± 1.1	10.1 ± 1.9	6.1 ± 0.7	4.9 ± 1.2
k_2 (10^{-12} cm^3 molecule^{-1} s^{-1})	30.9 ± 1.7	17.8 ± 0.6	14.9 ± 0.6	10.9 ± 1.1	6.0 ± 0.5	5.4 ± 0.7

[a] The lowest line contains the weighted average of the upper lines.

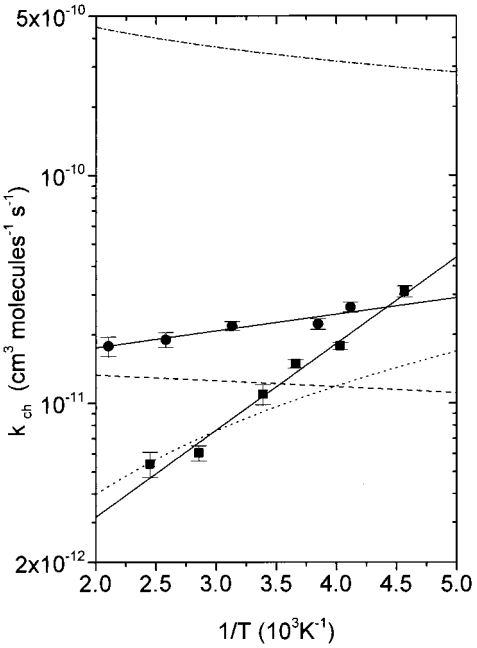

Figure 4. Arrhenius plot of k_{ch} for the reaction of the ethyl radical (●) and the *tert*-butyl radical (■) with NO. The solid lines correspond to Arrhenius fits to the data, and the collision limit for the reaction is represented by the dash−dotted line. The dashed and the dotted lines represent the reaction of CH_3 with NO,[8] where two extrapolation techniques to the high-pressure limit were used (Troe factorization, dotted line; inverse Laplace/master equation technique, dashed line).

and on selectivities. Polar effects are thought to lead to a correlation of the addition rate constants or the activation energies in plots against IP(R) − EA(X), the difference between the ionization potential of the radical and the electron affinity of the unsaturated reaction partner. The origin is a stabilizing interaction of the high-lying radical SOMO and the olefin LUMO frontier orbitals, which leads to a partial charge transfer from the radical to the acceptor LUMO in the transition state, accompanied by a corresponding lowering of its energy. The preexponential factor is assumed to be constant within a class of comparable reactions. Such correlations work reasonably well for the activated addition reactions of organic radicals to olefins in liquids.[34,35]

A similar correlation is found on the basis of the classical harpoon model, which assumes an initial electron transfer at a critical reaction distance where the Coulomb interaction between the newly formed ion pair R^+X^- equals IP(R) − EA(X). This process allows for an estimate of the Arrhenius preexponential factor, but it does not account for a temperature dependence other than $T^{1/2}$ as given by the relative velocity of the collision partners.

In view of this, it is curious that Paltenghi et al.[9] found a nearly linear plot of ln(k_{ch}) against IP(R) − EA(X) for the addition of alkyl radicals to O_2 and to O_3. The values for the reactions of alkyl radicals that were determined by μSR[2,3] fit on this plot as well, but a simple extension to reactions with NO and NO_2 (with values from literature and from the present work) is less satisfactory. Indeed, on the basis of the behavior shown in Figure 4 for the reactions with NO, it would seem fortuitous if the correlation applied, since there is a crossover of rate constants with temperature, whereas the sequence of IP − EA does not allow for such extreme temperature variations. Paltenghi et al.[9] successfully used the adiabatic channel model by Quack and Troe[36] in which they included a modified long-range potential relating to IP − EA, and good agreement with experimental rate constants was obtained. It was shown that the result is very sensitive to the shape of the long-range potential. The study did not address temperature dependence, however.

On the basis of transition-state theory, it has been possible to explain slightly negative activation energies for high-pressure limiting rate constants, but it appears to be nontrivial to obtain a quantitative understanding of the more negative values. There is obviously a pronounced energy dependence of the dynamics and thus of the cross section for addition reactions that occur on a shallow anisotropic attractive potential energy surface for that current theories do not always give a satisfactory answer. As pointed out by Troe, elementary reactions involving radicals and atoms with open shells may be influenced by electronic transitions between fine-structure components of the potential.[1] It has been suggested that in radical additions to NO an excited nondissociative triplet state of the adduct plays a crucial role.[10,13]

Conclusions

The additions of NO to the ethyl radical and to the *tert*-butyl radical have been investigated in the temperature range of 219−475 K and a pressure of 1.5 bar. For both reactions it is the first time that temperature-dependent kinetic data are reported. The present work confirms again that the muon spin relaxation technique competes well with more conventional gas kinetic methods.

Both reactions show a negative temperature dependence. The activation energy of the addition of the ethyl radical to NO is close to values that have been found for association reactions with O_2.[2,3] However, for the *tert*-butyl radical reaction with NO it is remarkably higher, revealing a more pronounced temperature dependence of the reaction cross section, which is possibly related to a competition between two attractive potential energy surfaces.

For the addition reaction of ethyl to NO, a room temperature rate constant was found that is about 100 times higher than the only comparable value of Pratt et al.[11] The present result fits well into a series of similar reactions and casts serious doubts on the earlier determination.

References and Notes

(1) Troe, J. *Ber. Bunsen-Ges. Phys. Chem.* **1994**, *98*, 1399. Troe, J. *Ber. Bunsen-Ges. Phys. Chem.* **1990**, *94*, 1183.

(2) Dilger, H.; Schwager, M.; Tregenna-Piggott, P. L. W.; Roduner, E.; Reid, I. D.; Arseneau, D. J.; Pan, J. J.; Senba, M.; Shelley, M.; Fleming, D. G. *J. Phys. Chem.* **1996,** *100*, 6561, 16445.

(3) Dilger, H.; Stolmár, M.; Tregenna-Piggott, P. L. W.; Roduner, E.; Reid, I. D. *Ber. Bunsen-Ges. Phys. Chem.* **1997,** *101*, 956.

(4) Walker, D. C. *Muon and Muonium Chemistry;* Cambridge University Press: Cambridge, 1983.

(5) Roduner, E. *The Positive Muon as a Probe in Free Radical Chemistry*; Lecture Notes in Chemistry 49; Springer-Verlag: Berlin, 1988.

(6) Fleming, D. G.; Pan, J. J.; Senba M.; Arseneau, D. J.; Kiefl, R. F.; Shelley, M.; Cox, S. F. J.; Percival, P. W.; Brodovitch, J.-C. *J. Chem. Phys.* **1996,** *105*, 7517.

(7) Pan, J. J.; Fleming, D. G.; Senba M.; Arseneau, D. J.; Snooks, R.; Baer, S.; Shelley, M.; Percival, P. W.; Brodovitch, J.-C.; Addison-Jones, B.; Wlodek, S.; Cox, S. F. J. *Hyperfine Interact.* **1994**, *87*, 865.

(8) McCaulley, J. A.; Anderson, S. M.; Jeffries, J. B.; Kaufman, F. *Chem. Phys. Lett.* **1985,** *63*, 180.

(9) Paltenghi P.; Ogryzlo, E. A.; Bayes, K. D. *J. Phys. Chem.* **1984**, *88*, 2595.

(10) Davies, J. W.; Green, N. J. B.; Pilling, M. J. *J. Chem. Soc., Faraday Trans.* **1991,** *87*, 2317.

(11) Pratt, G.; Veltman, I. *J. Chem. Soc., Faraday Trans. 1* **1976**, *72*, 2477.

(12) Kaiser, E. W. *J. Phys. Chem.* **1993**, *97*, 1167.

(13) Smith, I. W. M. *J. Chem. Soc., Faraday Trans.* **1991**, *87*, 2271.

(14) Pratt, G.; Veltman, I. *J. Chem. Soc., Faraday Trans 1* **1974**, *70*, 1840.

(15) Percival, P. W.; Brodovitch, J.-C.; Leung, S.-K.; Yu, D.; Kiefl, R. F.; Garner, D. M.; Arseneau, D. J.; Fleming, D. G.; Gonzalez, A.; Kempton, J. R.; Senba, M.; Venkateswaran, K.; Cox, S. F. J. *Chem. Phys. Lett.* **1989**, *163*, 241.

(16) Roduner, E.; Strub, W.; Burkhard, P.; Hochmann, J.; Percival, P. W.; Fischer, H.; Ramos, M.; Webster B. C. *Chem. Phys.* **1982**, *67*, 275.

(17) Percival, P. W.; Brodovitch, J.-C.; Leung, S.-K.; Yu, D.; Kiefl, R. F.; Luke, G. M.; Venkateswaran, K.; Cox, S. F. J. *Chem. Phys.* **1988**, *127*, 137.

(18) Senba, M.; Fleming, D. G.; Arseneau, D. J.; Garner, D. M.; Reid, I. D. *Phys. Rev.* **1989**, *A 39*, 3871.

(19) James, F.; Roos, M. *Comput. Phys. Commun.* **1975**, *10*, 343.

(20) Fleming, D. G.; Kiefl, R. F.; Garner, D. M.; Senba, M.; Gonzalez A. C.; Kempton, J. R.; Arseneau, D. J.; Venkateswaran, K.; Percival, P. W.; Brodovitch, J.-C.; Leung, S.-K.; Yu, D.; Cox, S. F. J. *Hyperfine Interact.* **1990**, *65*, 767.

(21) Senba, M. *Phys. Rev. A* **1995,** *52*, 4599.

(22) Dilger H.; Roduner, E.; Stolmár, M.; Reid, I. D.; Fleming, D. G.; Arseneau, D. J.; Pan, J. J.; Senba, M.; Shelley, M. *Hyperfine Interact.* **1997,** *106*, 137.

(23) Baulch, D. L.; Cobos, C. L.; Cox, R. A.; Frank, P.; Hayman, G.; Just, Th.; Kerr, J. A.; Murrells, T.; Pilling, M. J.; Troe, J.; Walker, R. W.; Warnatz, J. *J. Phys. Chem. Ref. Data* **1994**, *23*, 1026.

(24) Ley, L.; Masanet, J.; Caralp, F.; Lesclaux, R. *J. Phys. Chem.* **1995,** *99*, 1953.

(25) Dove, J. E.; Hippler, H.; Troe, J. *J. Chem. Phys.* **1985,** *82*, 1907.

(26) Hippler, H. *Ber. Bunsen-Ges. Phys. Chem.* **1985,** *89*, 303.

(27) Kerr, J. A.; Parsonage, M. J. *Evaluated Kinetic Data on Gas-Phase Addition Reactions*; Butterworth: London, 1972.

(28) Pan, J. J.; Fleming, D. G.; Senba M.; Arseneau, D. J.; Gonzalez A. J.; Kempton, J. R.; Fleming, D. G. *J. Phys. Chem.* **1995,** *99*, 17160.

(29) Garner, D. M.; Fleming, D. G.; Arseneau, D. J.; Senba, M.; Reid, I. D.; Mikula, R. J. *J. Chem. Phys.* **1990**, *93*, 1732.

(30) Collins, C. J.; Bowman, N. S. *Isotope Effects in Chemical Reactions;* Van Nostrand Reinhold Company: New York, 1970.

(31) MOPAC, Version 7.0.

(32) McMillen, D. F.; Golden, D. M. *Annu. Rev. Phys. Chem.* **1982**, *33*, 493.

(33) Wagner, A. F.; Slagle, I. R.; Sarzynski, D.; Gutman, D. *J. Phys. Chem.* **1990**, *94*, 1853.

(34) Fischer, H. *Subsituent Effects on Absolute Rate Constants and Arrhenius Parameters for the Addition of tert-Butyl Radicals to Alkenes*; In Viehe, H. G., et al., Eds.; *Substiuent Effects in Radical Chemistry*, NATO ASI Series; Kluwer Academic Publishers: Dordrecht, 1986; p 123.

(35) Beranek, I.; Fischer, H. *Polar Effects on Radical Addition Reactions: An Ambiphilic Radical*; In Minisci, F. Free Radicals in Synthesis and Biology, NATO ASI Series; Kluwer Academic Publishers: Dordrecht, 1989; p 303.

(36) Quack, M.; Troe, J. *Ber. Bunsen-Ges. Phys. Chem.* **1977**, *81*, 329.